Cancer Imaging (2013) **13(3),** 306–313
DOI: 10.1102/1470-7330.2013.0031

ORIGINAL ARTICLE

Monitoring targeted therapy using dual-energy CT: semi-automatic RECIST plus supplementary functional information by quantifying iodine uptake of melanoma metastases

M. Uhrig[a], M. Sedlmair[b], H.P. Schlemmer[a], J.C. Hassel[c], M. Ganten[a]

[a]*Department of Radiology, German Cancer Research Center, Im Neuenheimer Feld 280, Heidelberg, D-69120, Germany;* [b]*Siemens AG, Healthcare Sector, Siemensstr. 1, D-91301 Forchheim, Germany;* [c]*National Center for Tumor Diseases (NCT) Heidelberg, Im Neuenheimer Feld 460, D-69120 Heidelberg, Germany*

Corresponding address: Dr Monika Uhrig, MD, INF 280, Heidelberg, D-69120, Germany.
Email: m.uhrig@dkfz-heidelberg.de

Date accepted for publication 15 May 2013

Abstract

Aim: Supplementary functional information can contribute to assess response in targeted therapies. The aim of this study was to evaluate semi-automatic RECIST plus iodine uptake (IU) determination in melanoma metastases under BRAF inhibitor (vemurafenib) therapy using dual-energy computed tomography (DECT). **Methods:** Nine patients with stage IV melanoma treated with a BRAF inhibitor were included. Contrast-enhanced DECT was performed before and twice after treatment onset. Changes in tumor size were assessed according to RECIST. Quantification of IU (absolute value for total IU (mg) and volume-normalized IU (mg/ml)) was based on semi-automatic tumor volume segmentation. The decrease compared with baseline was calculated. **Results:** The mean change of RECIST diameter sum per patient was −47% at the first follow-up (FU), −56% at the second FU ($P<0.01$). The mean normalized IU per patient was −21% at the first FU ($P<0.2$) and −45% at the second FU ($P<0.01$). Total IU per patient, combining both normalized IU and volume, showed the most pronounced decrease: −89% at the first FU and −90% at the second FU ($P<0.01$). **Conclusion:** Semi-automatic RECIST plus IU quantification in DECT enables objective, easy and fast parameterization of tumor size and contrast medium uptake, thus providing 2 complementary pieces of information for response monitoring applicable in daily routine.

Keywords: *Drug monitoring; spiral computed tomography; targeted molecular therapy; melanoma; dual-energy computed tomography.*

Introduction

Targeted therapies are one of the most promising developments in cancer treatment; survival rates are increasing dramatically for some tumor entities[1]. For patients with unresectable or metastatic melanoma, there is an urgent need for innovative therapies because the incidence of melanoma is increasing worldwide[2] and the effects of conventional chemotherapy patients with stage IV[3] melanoma remains poor; the median survival time is less than a year[4]. Vemurafenib (Zelboraf, La Roche), a new targeted therapy for these patients, was approved in 2011 by the US Food and Drug Administration for the treatment of patients with unresectable or metastatic melanoma with the BRAF V600E-mutation[5]. The European Commission authorized this BRAF inhibitor in February 2012. BRAF is a cytoplasmic serine/threonine kinase in cellular signaling pathways[6]. About 40–60% of all patients with melanoma show a V600E-mutation in BRAF kinase, in most cases leading to substitution of glutamic acid by valine at codon 600[7]. Patients with this mutation can be successfully treated with vemurafenib, a small-molecule BRAF inhibitor[8].

Targeted therapies challenge therapy monitoring to provide an accurate and prompt response assessment to these new drugs[9]. A reliable and standardized methodology is essential, not only in clinical research but also in daily patient care. Response Evaluation Criteria in Solid

Tumors (RECIST) have been defined in order to approach such a standardized methodology. RECIST is based on the sum of one-dimensional measurements of the greatest diameter of the tumor and/or metastases[10]. But in contrast to general cytotoxic effects of standard chemotherapy leading to shrinkage of tumor size identifiable by RECIST, targeted therapies are designed to interfere with specific aberrant biological pathways involved in the tumorigenic process.

Alternative assessment criteria have been proposed, adding functional information to size-based monitoring. For example, the Choi criteria[11] were introduced for gastrointestinal stromal tumors (GIST) treated with imatinib mesylate; they combine both size and density measurements in computed tomography (CT). However, tumor response may also result in increased density because of intratumoral hemorrhage, which is observed, for example, during sorafenib therapy for hepatocellular carcinoma[12].

In a clinical phase I study of vemurafenib, the investigators were able to relate the altered tumor metabolism to decreased signal intensities on fluorodeoxyglucose (FDG)-positron emission tomography (PET). In 81% of patients, significant reduction of FDG uptake was observed 2 weeks after therapy onset, before tumor regression could be measured[6]. But the use of FDG-PET in monitoring tumor response is restricted due to high costs and limited availability. Consequently, for vemurafenib, as for most cancer treatments, response monitoring is performed by applying RECIST.

But a single response evaluation criterion may not be sufficient regarding developments such as necrosis without a change in tumor size under targeted therapies[13] leading to underestimation of response. Additional functional information, for example, on tumor vascularization, can contribute to therapy monitoring[14].

In clinical routine, radiologists evaluate tumor size as well as enhancement of contrast medium. Measuring size and comparing tumor diameters between FU examinations is standard, however validation of contrast medium enhancement is often a qualitative evaluation and far less objective than documenting lesion size. In multiphasic CT, comparisons between attenuation coefficients allow a semi-quantitative indicator for contrast agent enhancement[15] but also implicate increased radiation dose due to the additional unenhanced scan. The advanced dual-energy CT (DECT) technique overcomes this drawback.

DECT is a promising technique providing material-specific information. Two independent X-ray sources and corresponding detectors rotate around the patient. Materials with a considerable difference in Z values, such as tissue and iodine, can be separated by their spectral properties[16]. Using calibration measurements and image segmentation, the absolute value of iodine content in a certain volume can be calculated (VIU). Thus, in a single scan, DECT provides quantification of iodinated contrast agent uptake, objectively documenting in a single number the absolute amount of iodine in a lesion and avoiding a preceding unenhanced scan. In contrast to density measurements in terms of Hounsfield units (HU), iodine quantification is not influenced by tissue modifications such as necrosis and hemorrhage, which can alter attenuation in CT and mimic reduced or increased contrast agent uptake. Iodine uptake (IU), therefore, could be a new parameter directly related to vital and vascularized tumor tissue.

The purpose of this study is to improve tumor response monitoring of targeted therapies by evaluating the feasibility of semi-automatic RECIST evaluation with supplementary IU quantification in one step and to show the initial results from quantification of IU of melanoma metastases treated with the BRAF inhibitor vemurafenib.

Materials and methods

Patient population

Our institutional review board approved this retrospective study and patients gave informed consent. Consensus reading was performed by 2 radiologists, one of them with over 15 years of experience in oncologic imaging.

A total of 35 metastases (range 2–5 per patient) from 9 patients (3 males, 6 females, mean age 58 years, range 41–71 years) were examined with DECT before vemurafenib therapy twice after treatment onset between September 2010 and April 2012. Inclusion criteria were

- diagnosis of stage IV melanoma
- proof of V600E mutation
- treatment with vemurafenib
- baseline and 2 FU examinations at our institution with identical examination protocol
- presence of measurable target lesions

Mean time to first FU was 9 weeks (range 7–11 weeks) and 16 weeks to the second FU (range 13–20 weeks).

Data acquisition

The examination protocol included intravenous application of nonionic iodinated contrast medium (Imeron 300, Bracco) via an automated injector with the amount and flow rate adapted for body weight (Table 1). Contrast

Table 1 **Amount of contrast medium applied (Imeron 300, Bracco)**

Body weight (kg)	Volume of contrast medium (ml)	Flow rate (ml/s)
<55	85	3.1
55–65	115	3.5
65–90	130	4
>90	145	4.5

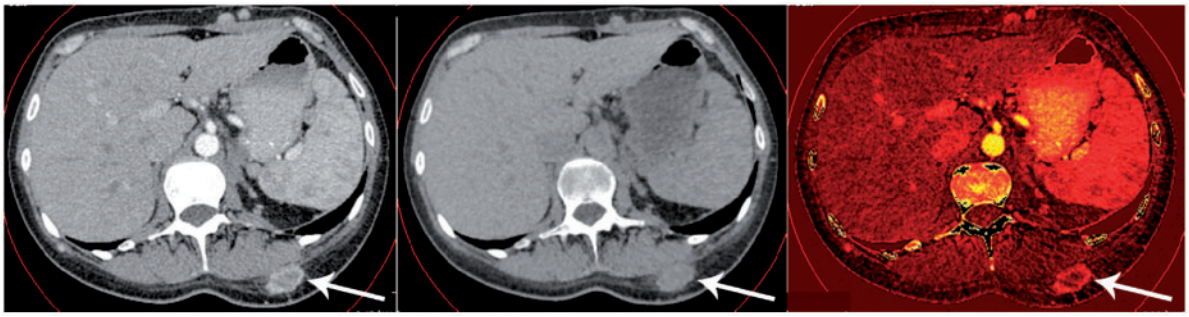

Figure 1 **Three visualization modes are available: common contrast-enhanced CT image (left), virtual unenhanced image (center) and iodine uptake (right), where amount of iodine uptake is color-coded for each voxel and displayed in a two-dimensional overview. Brighter red correlates with higher iodine content. Note the subcutaneous metastasis dorsal on the left with its inhomogeneous contrast medium enhancement.**

medium injection was triggered by attenuation measurements in a region of interest (ROI) placed in the abdominal aorta at the level of the liver. The arterial phase started 10 s after the cutoff value of 120 HU was detected (Bolus tracking technique), field of view was from neck to upper abdomen. Portal venous images were acquired 60 s after the arterial phase with a field of view from the upper abdomen to the proximal part of the upper leg.

Helical image acquisition was performed on a second-generation 128-row DECT (Siemens Somatom Definition Flash, Siemens Healthcare Sector, Forchheim, Germany), using 2 different tube voltages (100 kV and tin-filtered 140 kV, reference tube currents 200 mAs and 155 mAs) and online dose modulation (CARE Dose 4D, Siemens). The scan was acquired with a detector collimation of 32×0.6 mm in the caudocranial direction in the arterial phase (pitch 0.9) and in the craniocaudal direction in the portal venous phase (pitch 0.6) (the opposite scanning directions result in optimal contrast of pulmonary arteries in the arterial phase and optimal liver parenchyma contrast in the portal venous phase). With a weighting factor of 0.5, the 2 datasets from the 2 tube voltages were fused to virtual images corresponding to a 120-kV scan and were reconstructed into 1.5-mm slices (increment 1.0 mm) using a standard soft tissue reconstruction kernel (D20f smooth).

Data evaluation

Target lesions were selected according to RECIST and segmented semi-automatically using the Syngo.IPIPE software (Siemens Healthcare Sector, Forchheim, Germany). This algorithm segments a volume of interest after the user has drawn in the rough diameter of the lesion. In order to provide the best possible reproducibility, we abstained from manual correction of the segmented volumes and some lesions with diffuse margins had to be neglected because segmentation obviously did not match tumor spread.

Quantification of contrast medium enhancement with the LiverVNC application[16,17] was based on 'three-material decomposition' assuming the main components fat, soft tissue and iodine. In contrast with previous versions of LiverVNC, the package used for this study is able to transform spectral information of dual-energy data into absolute values of iodine content, based on calibration measurements performed by the manufacturer. For most lesions, uptake was calculated from images in the arterial phase. Exceptions are liver and spleen metastases, which are only definable in the portal venous phase.

Besides quantification, the software also provides visualization of IU by color-coding the amount of IU in each voxel and displaying the results in a two-dimensional overview (Figs. 1 and 2). By subtracting the iodine-related attenuation from the contrast-enhanced image, a virtual unenhanced scan is available (Fig. 1)[18–21].

RECIST diameter, total IU of the segmented volume (VIU; mg) and volume-normalized IU (mg/ml) were determined for the target lesions. For each patient, results from the target lesions were added to get the RECIST diameter sum, the sum of VIU and the sum of normalized IU. Statistical evaluation, using the paired *t* test, was performed for the individual lesions and patient based. Both perspectives were chosen because mixed responses are frequently observed under vemurafenib therapy, meaning that lesions can respond differently to therapy in each patient. All reported *P* values are two-sided and not corrected for multiple comparisons.

Results

Feasibility

Raw data had to be transferred to a dedicated workstation to evaluate IU. Uploading images into the local data bank took a few minutes. A graphical user interface allowed comparison of standard CT images, virtual native scan and visualization of IU, thus giving an overview of inhomogeneity of contrast agent enhancement (Figs. 1 and 3). Drawing a rough diameter for each

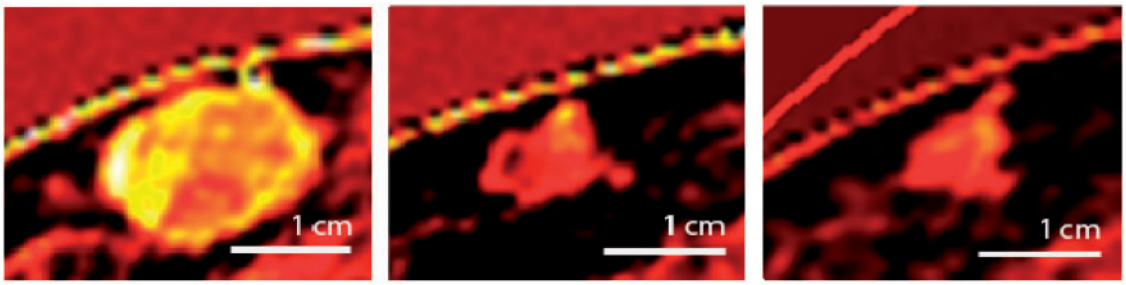

Figure 2 **Iodine uptake of a subcutaneous metastasis. Left: baseline, center, FU1; right: FU2.**

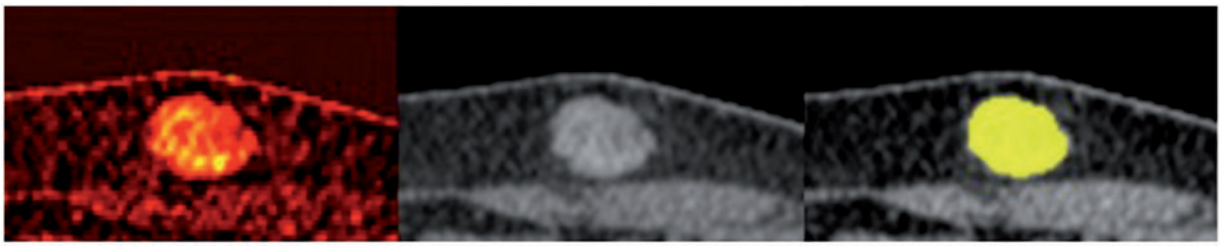

Figure 3 **Iodine uptake visualization of subcutaneous metastasis (left), demonstrating the inhomogeneous uptake of contrast medium. Center: mixed image, corresponding to a standard 120 kV contrast-enhanced image. Right: result of semi-automatic segmentation is displayed in yellow.**

Table 2 **Size and iodine uptake measurements for patient-based evaluation**

	RECIST (mm)	*P*	n-IU (mg/ml)	*P*	VIU (mg)	*P*
Baseline	69 (±30)		6.7 (±2.3)		16.8 (±8.5)	
ΔFU1	−33 (±13)	<0.01	−1.4 (±2.6)	<0.2	−15.0 (±8.0)	<0.01
ΔFU2	−39 (±11)	<0.01	−3.0 (±2.3)	<0.01	−15.1 (±6.2)	<0.01

Means with standard deviation are given. RECIST, sum of RECIST diameters of target lesions; n-IU, sum of normalized iodine uptake of target lesions; VIU, sum of total iodine uptake of the segmented target lesion volume; ΔFU, difference between follow-up and baseline.

target lesion was sufficient in most cases to start segmentation and calculation of RECIST diameter and IU. Segmentation failed in targets bounded by diffuse margins (e.g. liver lesions in arterial phase). Some metastases, especially if they were small after therapy, had to be segmented several times before segmentation matched tumor margin. To reduce potential bias, we first segmented the lesions before looking at the IU statistics.

Patient-based evaluation

Detailed results for RECIST and IU measurements for the different time points are given in Table 2.

RECIST

All patients were RECIST responders. Evaluation of baseline examinations revealed a mean RECIST diameter sum of 69 mm with a standard deviation (SD) of ±30 mm. The mean change in RECIST diameter sum per patient was −33 mm (SD ±13 mm) corresponding to −48% decrease at first FU ($P<0.01$) and −39 mm (SD ±11 mm) corresponding to −57% compared with baseline at second FU ($P<0.01$) (Fig. 4).

IU quantification

At the baseline examination, the mean sum of the normalized IU per patient was 6.7 mg/ml (SD ±2.3 mg/ml). The mean decrease was −1.4 mg/ml (SD ±2.6 mg/ml) corresponding to −21% at first FU ($P<0.2$) and −3 mg/ml (SD ±2.3 mg/ml) corresponding to −45% compared with baseline at the second FU ($P<0.01$). Looking at the individual patient data, we observed that only one patient showed increasing normalized IU sum at the first FU. Otherwise, all normalized IU sums had decreased compared with baseline (Fig. 5).

Mean VIU uptake sum per patient, combining both volume and normalized IU, was 16.8 mg (SD ±8.5 mg) at baseline and showed the most pronounced decrease of

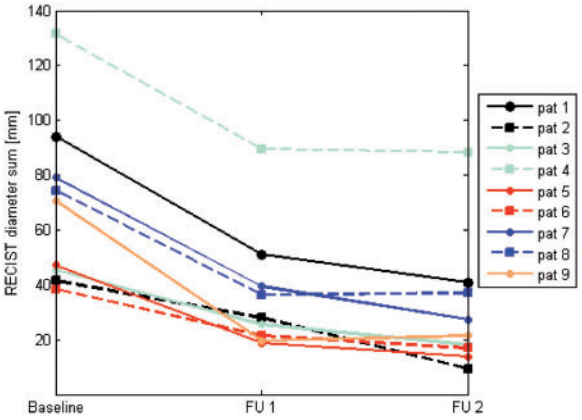

Figure 4 **Patient-based evaluation: course of RECIST-target diameter sum (mm). FU, follow-up.**

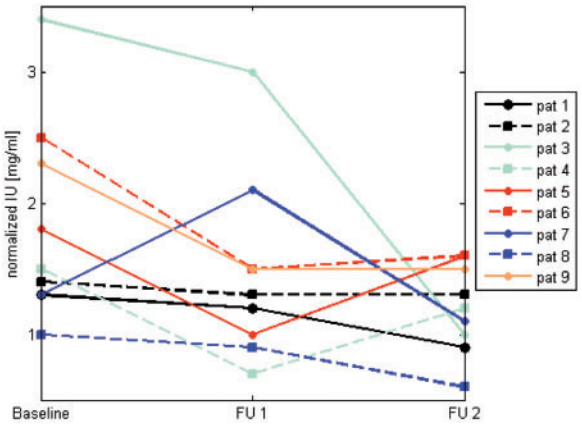

Figure 5 **Patient-based evaluation: course of volume-normalized iodine uptake (mg/ml), sum of targets for each patient is shown. FU, follow-up. IU, iodine uptake.**

the parameters assessed (Fig. 6). The mean difference from baseline was −15.0 mg (SD ±8.0 mg) corresponding to −89% at the first FU ($P<0.01$) and −15.1 mg (SD ±6.2 mg) corresponding to −90% ($P<0.01$) at the second FU.

IU measurements did not indicate response earlier compared with RECIST in any patient.

Lesion-based evaluation

Detailed results for RECIST and IU measurements for the different time points are given in Table 3.

RECIST

The mean RECIST diameter of the lesions at baseline was 18 mm (SD ±6 mm). A decrease of −8 mm (SD ±4 mm) corresponding to −44% was observed at the first FU ($P<0.01$) and −10 mm (SD ±5 mm)

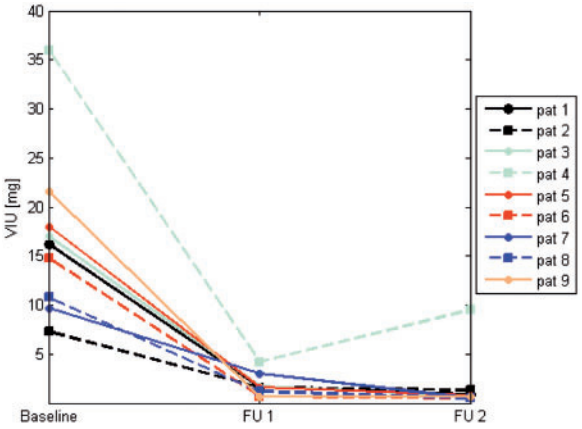

Figure 6 **Patient-based evaluation: course of total iodine uptake of the segmented volume (VIU) (mg), sum of targets for each patient is shown. FU, follow-up.**

corresponding to −56% compared with baseline at the second FU ($P<0.01$).

IU quantification

At baseline, the mean normalized IU per lesion was 1.7 mg/ml (SD ±1 mg/ml). It diminished −0.4 mg/ml (SD ±1.2 mg/ml) corresponding to −24% at the first FU ($P<0.1$) and −0.8 mg/ml (SD ±1.1 mg/ml) corresponding to −47% compared with baseline at the second FU ($P<0.01$).

Mean VIU uptake per lesion was 4.3 mg at baseline (SD ±4 mg). Similar to the patient-based evaluation, the most pronounced decrease was −3.9 mg (SD ±3.9 mg) corresponding to −91% at first FU ($P<0.01$), with no further significant decrease at second FU.

Radiation exposure

The mean computed tomography dose index (CTDI) per examination including neck, chest, abdomen and pelvis was 29 mGy (SD ±4 mGy), mean dose length product (DLP) per examination was 1518 mGy cm (SD ±188 mGy cm). Both values do not exceed the reference values given by the German Federal Office for Radiation Protection (52 mGy for CTDI and 1750 mGy cm for DLP for a CT examination including chest, abdomen and pelvis)[22].

Discussion

Tumor response monitoring of targeted therapies is a challenging and developing issue, considering that the action of these drugs is more cytostatic than cytotoxic. It is likely that size-based classification systems such as RECIST underestimate tumor response to targeted therapy[14].

Table 3 **Size and iodine uptake measurements for lesion-based evaluation**

	RECIST (mm)	*P*	n-IU (mg/ml)	*P*	VIU (mg)	*P*
Baseline	18 (±6)		1.7 (±1.0)		4.3 (±4.0)	
ΔFU1	−8 (±4)	<0.01	−0.4 (±1.2)	<0.1	−3.9 (±3.9)	<0.01
ΔFU2	−10 (±5)	<0.01	−0.8 (±1.1)	<0.01	−3.9 (±4.0)	<0.01

Means with standard deviation are given. RECIST, RECIST diameter per target; n-IU, normalized iodine uptake per target; VIU, total iodine uptake of the segmented target lesion volume; ΔFU, difference between follow-up and baseline.

Ongoing developments in targeted therapies increase the need for a practical, objective and reproducible biomarker for monitoring tumor response.

For a subset of drugs, evaluation criteria aligned to specific therapy effects already exist[23]. This is not true for BRAF inhibitor therapy for which RECIST has been the most common monitoring system[24]. In a clinical phase I study of vemurafenib, an additional PET scan was performed; in 81% of patients, a significant reduction in FDG uptake was observed 2 weeks after therapy onset, before tumor regression could be measured[6].

Compared with PET, the standard CT examination is fast and low cost and therefore used extensively for monitoring tumor response, but it includes less functional information. Supplementary biological information from the dual-energy technique has the potential to fill this gap.

IU is a new assessment parameter provided by DECT and is assumed to reflect vital tumor burden by measuring the IU of active tumor. Iodinated contrast medium in lesions is mainly brought by arterial blood perfusion of viable tumor. Reflecting this biological information about the tumor, it could be a promising tool for evaluating new targeted therapies.

In this study, we demonstrated the feasibility of IU quantification in BRAF inhibitor treatment of melanoma and presented the first results for patients undergoing vemurafenib therapy. The quantification of IU showed a decrease for all iodine parameters; VIU uptake per patient showed the most pronounced decrease.

The reduction in volume-normalized IU at first FU was not significant although a significant size reduction was observed. One reason could be the small sample size of 9 patients. Another possibility is a potential partial volume effect; a significant decrease in lesion size means that many small metastases have to be segmented. Small parts of the surrounding tissue close to the tumor margin can be accidentally segmented with the target, and there is no change in IU in this healthy tissue. If the actual metastasis is already very small, the influence of this segmentation inaccuracy is higher compared with large lesions.

The parameter VIU, which has not been used up to now in studies using DECT for response monitoring, not only describes reduced IU but also size shrinkage; consequently a more pronounced diminishment compared with volume-normalized IU was observed. VIU delivers a single number representing 2 main characteristics of tumors: volume and contrast agent enhancement.

A relationship between tumor angiogenesis and contrast enhancement on CT was demonstrated by Miles et al.[25]. Analogously, assuming that iodine does not occur in detectable amounts in normal tissue and mimics contrast agent, the diminishment of volume-normalized IU observed in our study is probably caused by reduced vascularization of metastases under vemurafenib therapy. This fits well with the mechanisms described for BRAF inhibitors: Oncogenic BRAF kinase is an important stimulator of metabolic activity[26–28], so inhibiting this enzyme by vemurafenib results in modification of metabolism.

Earlier attempts at contrast agent quantification have used DECT and multiphasic CT scans[15]. In contrast to DECT, multiphasic CT requires an additional unenhanced scan. The new generation of dual-energy scanners using tin-filter technology allows scanning protocols with radiation doses equivalent to single energy scans, therefore our DECT multiparametric therapy monitoring approach is feasible at a lower radiation dose than multiphasic CT[29,30].

An indirect method of iodine quantification with DECT in therapy monitoring was described by Apfaltrer et al.[31]. These authors could correlate iodine-related attenuation for GISTs with the Choi criteria, without investigating absolute IU (mg). In contrast to our study, they used a non-standardized two-dimensional ROI. A similar approach for semi-quantitative iodine measurements in GIST using a manually driven ROI around the margin of the entire tumor describes an inconclusive relationship between RECIST/Choi criteria and IU[32].

Direct quantification of IU by DECT in phantoms and renal lesions was performed by Chandarana et al.[33]. They showed that accurate iodine quantification is possible. IU values were normalized to volume using a freehand two-dimensional ROI, similar to Apfaltrer et al.[31].

All these studies have in common the methodological approach of defining a representative but non-standardized two-dimensional tumor region. Whenever ROI measurements are chosen, there is the challenge of appropriate ROI placement in heterogeneous tissue. We could avoid this limitation by performing whole-lesion segmentation.

Compared with the qualitative evaluation of enhancement used in clinical routine, IU quantification is more objective. Measurements of attenuation in CT images are

often used as an indicator of IU. But in contrast to IU quantification, tissue modifications such as necrosis, edema and hemorrhage cannot be separated from increasing or decreasing vascularity as both lead to altered HU units. By contrast, IU is able to provide vascularization information based on displaying the volumetric distribution of iodinated contrast medium, regardless of the heterogeneous necrosis, edema, hemorrhage and volume changes caused by targeted therapy or tumor progression. With DECT and the semi-automatic postprocessing technique, IU measurements as a biomarker for tumor response are robust and easy to perform.

One of the major limitations of our study is the small sample size. However, the number was sufficient for a feasibility evaluation. In addition, the choice of lesions was limited; not every metastasis could be depicted as a target because segmentation did not match tumor extent in the presence of diffuse margins. Some lesions had to be segmented several times until they matched the tumor margins sufficiently. As a consequence of this study, the software will be improved to overcome these limitations.

Liver and spleen lesions were hardly definable in the arterial phase, consequently we evaluated metastases in these organs in the portal venous phase. As melanoma metastases are known to be hypervascularized, it would be more consistent to measure their uptake in the arterial phase. Nevertheless we could see a decrease in IU.

Changes in iodine concentration depend not only on tumor vascularization. Contrast agent dose and injection rate for an individual were not altered between FU examinations, but normalization as proposed in other studies[32], for example, using an ROI placed in the aorta[33], was not performed in our evaluation. In addition to the contrast agent injection parameter, there are other influencing factors not investigated in our study such as varying cardiac output or permeability of vessels.

In 81% of patients treated with vemurafenib, Bollag et al.[6] observed a significant reduction in FDG uptake after 2 weeks, before tumor size regression could be measured. In our study, the first FU examination of patients was several weeks after therapy onset and we eventually missed tumor stages characterized by reduced vascularization at constant lesion size. Compared with PET examinations, IU quantification in DECT is fast and low cost, so it would be worth performing a prospective study to correlate FDG and IU and investigate if both methods provide similar information about tumor metabolism.

In future studies survival time and tumor markers should be correlated with IU quantification to evaluate its value as a prediction parameter.

Conclusion

Semi-automatic IU quantification enables objective, easy and fast parameterization of tumor size and contrast medium uptake, thus providing 2 complementary pieces of information for response monitoring applicable in daily routine. Feasibility has been shown for patients with melanoma under BRAF inhibitor therapy and the first results indicate a significant decrease in IU in RECIST responders. Future studies including correlation of IU with biomarkers and comparisons with FDG uptake will demonstrate if IU quantification can monitor response to targeted therapies in patients with melanoma earlier and more reliably compared with RECIST.

Conflict of interest

The authors have no conflicts of interest to declare.

References

[1] Gray-Schopfer V, Wellbrock C, Marais R. Melanoma biology and new targeted therapy. Nature 2007; 445: 851–857. doi:10.1038/nature05661. PMid:17314971.

[2] Garbe C, Leiter U. Melanoma epidemiology and trends. Clin Dermatol 2009; 27: 3–9. doi:10.1016/j.clindermatol.2008.09.001. PMid:19095149.

[3] Balch CM, Gershenwald JE, Soong SJ, et al. Final version of 2009 AJCC melanoma staging and classification. J Clin Oncol 2009; 27: 6199–6206. doi:10.1200/JCO.2009.23.4799. PMid:19917835.

[4] Garbe C, Eigentler TK, Keilholz U, Hauschild A, Kirkwood JM. Systematic review of medical treatment in melanoma: current status and future prospects. Oncologist 2011; 16: 5–24. doi:10.1634/theoncologist.2010-0190. PMid:21212434.

[5] Flaherty KT, Yasothan U, Kirkpatrick P. Vemurafenib. Nat Rev Drug Discov 2011; 10: 811–812. doi:10.1038/nrd3579. PMid:22037033.

[6] Bollag G, Hirth P, Tsai J, et al. Clinical efficacy of a RAF inhibitor needs broad target blockade in BRAF-mutant melanoma. Nature 2010; 467: 596–599. doi:10.1038/nature09454. PMid:20823850.

[7] Davies H, Bignell GR, Cox C, et al. Mutations of the BRAF gene in human cancer. Nature 2002; 417: 949–954. doi:10.1038/nature00766. PMid:12068308.

[8] Flaherty KT, Puzanov I, Kim KB, et al. Inhibition of mutated, activated BRAF in metastatic melanoma. N Engl J Med 2010; 363: 809–819. doi:10.1056/NEJMoa1002011. PMid:20818844.

[9] Figueiras RG, Padhani AR, Goh VJ, et al. Novel oncologic drugs: what they do and how they affect images. Radiographics 2011; 31: 2059–2091. doi:10.1148/rg.317115108. PMid:22084189.

[10] Eisenhauer EA, Therasse P, Bogaerts J, et al. New response evaluation criteria in solid tumours: revised RECIST guideline (version 1.1). Eur J Cancer 2009; 45: 228–247. doi:10.1016/j.ejca.2008.10.026. PMid:19097774.

[11] Choi H. Response evaluation of gastrointestinal stromal tumors. Oncologist 2008; 13(Suppl 2): 4–7. doi:10.1634/theoncologist.13-S2-4. PMid:18434631.

[12] Rombola F, Caravetta A, Mollo F, Spinoso A, Peluso L, Guarino R. Sorafenib, risk of bleeding and spontaneous rupture of hepatocellular carcinoma. A clinical case. Acta Medica (Hradec Kralove) 2011; 54: 177–179.

[13] Faivre S, Demetri G, Sargent W, Raymond E. Molecular basis for sunitinib efficacy and future clinical development. Nat Rev Drug Discov 2007; 6: 734–745. doi:10.1038/nrd2380. PMid:17690708.

[14] Shanbhogue AK, Karnad AB, Prasad SR. Tumor response evaluation in oncology: current update. J Comput Assist Tomogr 2010; 34: 479–484. doi:10.1097/RCT.0b013e3181db2670. PMid:20657213.

[15] Joo I, Lee JM, Kim KW, Klotz E, Han JK, Choi BI. Liver metastases on quantitative color mapping of the arterial enhancement fraction from multiphasic CT scans: evaluation of the hemodynamic features and correlation with the chemotherapy response.

Eur J Radiol 2011; 80: e278–283. doi:10.1016/j.ejrad.2010.12.002. PMid:21251785.

[16] Johnson TR, Krauss B, Sedlmair M, et al. Material differentiation by dual energy CT: initial experience. Eur Radiol 2007; 17: 1510–1517. doi:10.1007/s00330-006-0517-6. PMid:17151859.

[17] Petersilka M, Bruder H, Krauss B, Stierstorfer K, Flohr TG. Technical principles of dual source CT. Eur J Radiol 2008; 68: 362–368. doi:10.1016/j.ejrad.2008.08.013. PMid:18842371.

[18] Graser A, Johnson TR, Hecht EM, et al. Dual-energy CT in patients suspected of having renal masses: can virtual nonenhanced images replace true nonenhanced images? Radiology 2009; 252: 433–440. doi:10.1148/radiol.2522080557. PMid:19487466.

[19] Graser A, Johnson TR, Chandarana H, Macari M. Dual energy CT: preliminary observations and potential clinical applications in the abdomen. Eur Radiol 2009; 19: 13–23. doi:10.1007/s00330-008-1122-7. PMid:18677487.

[20] Okada M, Kim T, Murakami T. Hepatocellular nodules in liver cirrhosis: state of the art CT evaluation (perfusion CT/volume helical shuttle scan/dual-energy CT, etc.). Abdom Imaging 2011; 36: 273–281. doi:10.1007/s00261-011-9684-2. PMid:21267563.

[21] Lee SH, Lee JM, Kim KW, et al. Dual-energy computed tomography to assess tumor response to hepatic radiofrequency ablation: potential diagnostic value of virtual noncontrast images and iodine maps. Invest Radiol 2011; 46: 77–84. doi:10.1097/RLI.0b013e3181f23fcd. PMid:20856125.

[22] Bundesamt für Strahlenschutz: Bekanntmachung der aktualisierten diagnostischen Referenzwerte für diagnostische und interventionelle Röntgenuntersuchungen, http://www.bfs.de/de/ion/medizin/diagnostik/referenzwerte.html.

[23] Wolchok JD, Hoos A, O'Day S, et al. Guidelines for the evaluation of immune therapy activity in solid tumors: immune-related response criteria. Clin Cancer Res 2009; 15: 7412–7420. doi:10.1158/1078-0432.CCR-09-1624. PMid:19934295.

[24] Chapman PB, Hauschild A, Robert C, et al. Improved survival with vemurafenib in melanoma with BRAF V600E mutation. N Engl J Med 2011; 364: 2507–2516. doi:10.1056/NEJMoa1103782. PMid:21639808.

[25] Miles KA, Cuenod CA. Multidetector computed tomography in oncology CT perfusion imaging. London, UK: Informa Healthcare; 2007.

[26] Esteve-Puig R, Canals F, Colome N, Merlino G, Recio JA. Uncoupling of the LKB1-AMPKalpha energy sensor pathway by growth factors and oncogenic BRAF. PLoS One 2009; 4: e4771. doi:10.1371/journal.pone.0004771. PMid:19274086.

[27] Zheng B, Jeong JH, Asara JM, et al. Oncogenic B-RAF negatively regulates the tumor suppressor LKB1 to promote melanoma cell proliferation. Mol Cell 2009; 33: 237–247. doi:10.1016/j.molcel.2008.12.026. PMid:19187764.

[28] Wan PT, Garnett MJ, Roe SM, et al. Mechanism of activation of the RAF-ERK signaling pathway by oncogenic mutations of B-RAF. Cell 2004; 116: 855–867. doi:10.1016/S0092-8674(04)00215-6. PMid:15035987.

[29] Mangold S, Thomas C, Fenchel M, et al. Virtual nonenhanced dual-energy ct urography with tin-filter technology: determinants of detection of urinary calculi in the renal collecting system. Radiology 2012; 264: 119–125. doi:10.1148/radiol.12110851. PMid:22570506.

[30] Guggenberger R, Gnannt R, Hodler J, et al. Diagnostic performance of dual-energy CT for the detection of traumatic bone marrow lesions in the ankle: comparison with MR imaging. Radiology 2012; 264: 164–173. doi:10.1148/radiol.12112217. PMid:22570505.

[31] Apfaltrer P, Meyer M, Meier C, et al. Contrast-enhanced dual-energy CT of gastrointestinal stromal tumors: is iodine-related attenuation a potential indicator of tumor response? Invest Radiol 2012; 47: 65–70. doi:10.1097/RLI.0b013e31823003d2. PMid:21934517.

[32] Schramm N, Schlemmer M, Englhart E, et al. Dual energy CT for monitoring targeted therapies in patients with advanced gastrointestinal stromal tumor: initial results. Curr Pharm Biotechnol 2011; 12: 547–557. doi:10.2174/138920111795164066. PMid:21342100.

[33] Chandarana H, Megibow AJ, Cohen BA, et al. Iodine quantification with dual-energy CT: phantom study and preliminary experience with renal masses. AJR Am J Roentgenol 2011; 196: W693–700. doi:10.2214/AJR.10.5541. PMid:21606256.